NUCL SCI TECH (2017) 28:142
DOI 10.1007/s41365-017-0301-0

Numerical and experimental analysis of AC loss for CFETR CS model coil

Wei Zhou[1] · Xin-Yu Fang[2] · Jin Fang[1] · Yan-Chao Liu[1] · Bo Liu[3]

Received: 21 November 2016 / Revised: 23 December 2016 / Accepted: 7 January 2017 / Published online: 6 September 2017

Abstract The central solenoid (CS) is an important component of China Fusion Engineering Test Reactor, for producing, forming and stabilizing plasma in the superconducting tokamak. It is a complicated work to design and manufacture the large superconducting CS magnet, so it is meaningful to design a central solenoid model coil (CSMC) and analyze its electromagnetic properties in advance. In this paper, the structure, design parameters and magnetic field distribution of the CS model coil are discussed. The peak power of radial and axial turn conductors and time bucket loss are analyzed by using piecewise-linear method. The CSMC AC loss with different Nb_3Sn CICCs and AC loss of ITER CS coil are compared. The special electrometric method to measure AC loss of the CS model coil for future reference is presented.

Keywords CFETR CS model coil · AC loss · Experimental system

✉ Jin Fang
zhouwei910545@126.com

[1] School of Electrical Engineering, Beijing Jiaotong University, Beijing 100044, China

[2] Department of Electrical and Computer Engineering, University of Victoria, Victoria, BC V8W2Y2, Canada

[3] Institute of Plasma Physics, Chinese Academy of Sciences, Hefei 230031, China

1 Introduction

China Fusion Engineering Test Reactor (CFETR) is a new tokamak device under concept design, in major radius of 5.7 m and minor radius of 1.6 m. Based on superconducting magnet technology, it is envisioned to provide 200 MW fusion power with the designed duty cycle time of 0.3–0.5 [1]. It is acknowledged that the preliminary design of CFETR is relied on physical and technical bases of the International Thermonuclear Experimental Reactor (ITER) and Experimental Advanced Superconducting Tokamak (EAST). In Table 1, design parameters are compared between the ITER and CFETR [2, 3]. Like other tokamak devices, the CFETR magnet system consists of 16 toroidal field (TF) coils, 6 central solenoid (CS) coils and 6 poloidal field (PF) coils. The TF system has 16 identical D-shape coils to produce strong toroidal magnetic field to confine the plasma. Design by integral method, all the CS and PF coils contribute to the heating and equilibrium process. Configuration of the PF coils has the ability to explore new equilibrium magnetic shape, such as super-X and snowflake shape, in addition to the ITER-like diverter shape [4].

The CFETR is in development at Institute of Plasma Physics, Chinese Academy of Science. Our work is to design a central solenoid model coil (CSMC) and analyze its electromagnetic properties for developing the CFETR CSMC. The tasks include: electromagnetic and mechanical analysis [5], cabling technology of Nb_3Sn conductor [6] and mechanical performance of designed insulation for the CSMC [7], and numerical model for quench simulation of CSMC conductor [8].

AC loss measurements for ITER and KSTAR CSMC have been studied by many authors [9–11]. As an indicator

Table 1 The main technical parameters of CFETR and ITER

Parameters	CFETR	ITER
Plasma current (I_p) (MA)	8.5–10	15
Major radius of plasma (R) (m)	5.7	6.2
Minor radius of plasma (r) (m)	1.6	2.0
Central magnetic field (B_t) (T)	4.5/5	5.3
Triangle deformation	0.4	0.33/0.48
Elongation ratio	1.8	1.7/1.85

of the stability for practical application of large superconducting fusion experiment, AC loss aggravates the burden of refrigeration system, hence the importance of its calculation and measurement for CFETR magnets. Numerical AC loss analysis for the CSMC was preliminary calculated [12], but the AC loss results of different Nb_3Sn cable-in-conduit conductors (CICCs) should be compared and discussed. The NbTi CICCs for CSMC2 of CFETR is to use the ITER PF5 conductors. The pattern of Nb_3Sn-based coil shall be designed on basis of experiments, but some conductors are preferred, such as ITER-like CS and TF conductors. So, it is necessary to compare the AC loss of these types of Nb_3Sn conductors.

In this paper, based on updated design parameters [5], the AC losses are calculated and compared, including hysteresis loss and coupling loss of different Nb_3Sn CICCs. A special system is proposed for measuring the AC loss and providing experimental basis for the CSMC.

2 Structure and magnetic field distribution

The CSMC design has a maximum magnetic field of 12 T and the top ramp rate of 1.5 T/s, which require extremely high operation current. The model coil consists of two concentric coil modules: a Nb_3Sn module in high field area (CSMC1) and a NbTi module in low field area (CSMC2). Considering the limitation of manufacturing technology, the CSMC1 cannot be wound by over 1000 m Nb_3Sn conductor, so it is divided into inner (CSMC1-1) and outer (CSMC1-2) Nb_3Sn coils. The structure parameters of the CSMC are given in Table 2 [5]. The "$49^2 \times \Phi32.6$" means that the stainless steel jacket is of a 49 mm × 49 mm cross section and the Nb_3Sn conductor is 32.6 mm in diameter, and $51.9^2 \times \Phi35.3$ can be described similarly.

Electromagnetic properties of the CSMC are analyzed with the finite element method software of COMSOL, using the size data in Table 2, and knowing the operation current of 48.3 kA for plasma equilibrium configuration. As shown in Fig. 1, the maximum magnetic field (11.7 T) of CSMC1 occurs at its middle, and the maximum magnetic field (5.7 T) of CSMC2 occurs at its upper part, while the corresponding design requirements in Table 2 are 12 and 5.8 T.

3 Conductors and operation current

3.1 Parameters of selected conductors

According to the design, main parameters of the NbTi-based coil (CSMC2) are the same as those of ITER PF5. The pattern of Nb_3Sn-based coil (CSMC1) shall be similar to ITER conductors, too, so it is necessary to compare AC losses of several types of Nb_3Sn conductors. CSMC1 shall be wound with CNTF4 (of short twist pitches), CSKO1 (of short twist pitches) and CSJA3 (of original twist pitch). Peak powers of the conductor units (a total of 460 conductor units, from Fig. 1), and the hysteresis loss and coupling loss of CSMC1, are calculated, and the results are compared. Peak power of the conductor units, and hysteresis loss and coupling loss of CSMC2, wound as ITER PF5, are analyzed, too. The main information for CNTF4, CSKO1, CSJA3 and ITER PF5 conductors is described as follows:

The CNTF4 conductor is based on Nb_3Sn internal-tin strands, manufactured by Western Superconducting Technologies Company (WST). Cabling and jacketing operations are performed in collaboration between Institute of Plasma Physics and Baosheng Company in China according to a layout determined by ITER TF conductor specification [13].

The CSKO1 and CSJA3 conductors are designed and manufactured by JAPAN Atomic Energy Agency (JAEA). The CS conductor consists of 576 Cr-plated Nb_3Sn strands, 288 Cr-plated Cu strands, a stainless steel central spiral, stainless steel wraps and a stainless steel round-in-square jacket. As shown in Table 3, the twist pitches from the first to fourth CSKO1 are shorter than those of CSJA3. So CSKO1 is called short twist pitch (STP) conductor and CSJA3 is regarded as original twist pitch conductor. The other difference is that the CSKO1 conductor consists of internal-tin Nb_3Sn strands, while CSJA3 conductor consists of bronze-route Nb_3Sn strands.

Institute of Plasma Physics is the supplier of the ITER PF5 conductors for the ITER project. The NbTi superconducting strands of PF5 were supplied by WST, and the parameters are listed in Table 3. Typical cross sections and main parameters of the strands and conductors for AC loss calculation are shown in Fig. 2 and Table 3 [14–16].

Table 2 Main structure parameters of CFETR CS model coil (maximum current, 48.3 kA; inductance, 322.7 mH)

Parameters	CSMC1-1	CSMC1-2	CSMC2
Conductor type	Nb_3Sn	Nb_3Sn	NbTi
Conductor size (mm)	$49^2 \times \Phi 32.6$	$49^2 \times \Phi 32.6$	$51.9^2 \times \Phi 35.3$
Radial turns	4	4	10
Axial turns	30	30	22
Inside radius (mm)	750.0	976.2	1242.4
Outside radius (mm)	953.8	1180.0	1784.8
Height (mm)	1545.4	1545.4	1196.4
Conductor length (m)	642	813	2092
Maximum field (T)	12	8.4	5.8

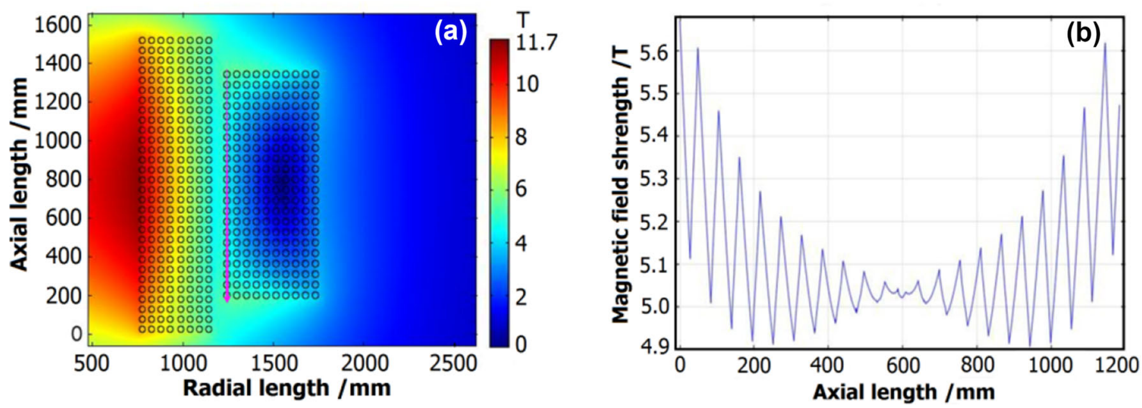

Fig. 1 (Color online) Magnetic field distribution (**a**) of the CSMC and magnetic field amplitude (**b**) along the *arrow* (**a**), at the maximum current of 48.3 kA by the COMSOL code. The *arrow* starts at the top conductor ($x = 0$) and ends at the *bottom* conductor ($x = 1196.4$ mm, the height of CSMC2)

3.2 Operation current waveform of CSMC

Due to the similar plasma position and operation mode between ITER and CFETR, the CSMC has similar current waveform to ITER CS coil. In this paper, CS2U simplified current is chosen based on ITER CS as an example, as shown in Fig. 3 [17]. For calculation convenience, piece-wise-linear method was used. The whole current waveform was divided into 19 segments, and each segment can be regarded as a straight line with same dI/dt which simplifies the calculation process.

4 Results and discussion

Equations (1) and (2) are used to calculate AC loss (in W/m^3) including coupling loss Q_c and hysteresis loss Q_h [18, 19]:

$$Q_c = (n\tau/\mu_0)(\partial B/\partial t)^2, \quad (1)$$

$$Q_h = (2/3\pi)J_c d_{eff}\left[1 + (I_{tr}/I_c)^2\right](\partial B/\partial t), \quad (2)$$

where $n\tau$ is coupling time constant of the conductor which can be measured in advance, μ_0 is permeability of vacuum, $\partial B/\partial t$ is the rate of change of magnetic field which related to the rate of change of operation current, d_{eff} is the effective filament diameter, I_{tr} is transport current of CICC, and I_c and J_c are critical current and critical current density of the conductor which can be obtained by L. Bottura's model [20, 21].

Coupling and hysteresis losses of the CSMC can be thus numerically analyzed with known operation current and the parameters of CICCs. It should be noted that there is a very small eddy current loss in the metal structural components of CSMC which can be simulated by 3-D ANSYS/EMAG code [22]. In this paper, we neglected the eddy current loss.

4.1 Hysteresis loss of CSMC1 and CSMC2

By using COMSOL, $\partial B/\partial t$, I_c and J_c are calculated. Hysteresis loss of CSMC1 made of CNTF4, CSKO1 and CSJA3 conductors, and CSMC2 made of ITER PF5 conductor, are then obtained. The results are given in Table 4 (the left half). The hysteresis loss of the CNTF4, CSKO1

Table 3 Summary of main parameters of selected strands and conductors [14–16]

Item	CNTF4	CSKO1	CSJA3	ITER PF5
Nb_3Sn/NbTi strand parameters				
Strand diameter/mm	0.820–0.821	0.82	0.83	0.73
Critical current/A	230.2–265.0 at 4.2 K/12 T	274 at 4.2 K/12 T	>260 at 4.2 K/12 T	>356 at 4.2 K/5 T
Copper-to-non-copper	0.92–1.037	1	0.99–1.01	2.268
Hysteresis loss (±3T)/mJ cm^{-3}	379.5–591.6	<500	<500	40.5
Conductor parameters				
Conductor diameter/mm	43.75	49	49	35.3–36.2
Cabling layout	[(2SC + 1Cu) × 3×5 × 5 + Cu core] × 6	(2SC + 1Cu) × 3×4 × 4×6	(2SC + 1Cu) × 3×4 × 4×6	[(3SC × 4×4 × 4) + 1 Cu core] × 6
Twist pitch/mm	84/145/194/308/421	23/49/80/154/450	45/85/145/250/450	45/85/145/250/450
Coupling time constant/ms	130	60.6	90	65

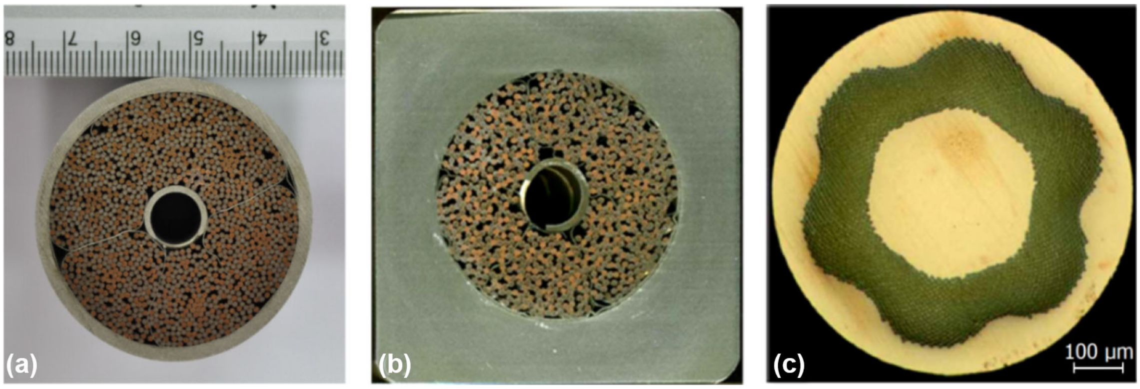

Fig. 2 (Color online) Cross sections of CNTF4 CIC (**a**) and CSJA3 CIC conductors (**b**) for CSMC1, and the ITER PF5 NbTi strands for CSMC2 (**c**)

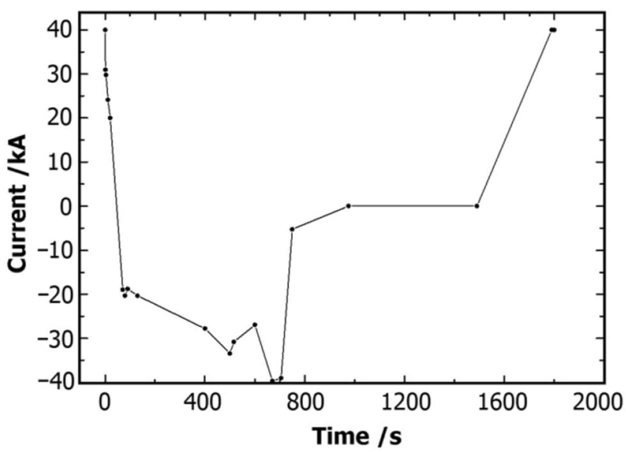

Fig. 3 CS2U simplified current waveform for calculation of the CSMC

and CSJA3-based CSMC1, and ITER PF5-based CSMC2, is 657.2, 504.2, 454.6 and 56.4 kJ, respectively. The fifth time bucket (T5) and eighteenth time bucket (T18) are of the highest hysteresis loss because AC loss per cycle (J/cycle) depends on the rate of magnetic field or the input current rate (777.6 A/s for T5 and 133.3 A/s for T18), and on the duration of time bucket (50 s for T5 and 300 s for T18).

4.2 Coupling loss of CSMC1 and CSMC2

The calculated coupling loss of CSMC1 made of CNTF4, CSKO1 and CSJA3 conductors, and CSMC2 made of ITER PF5 conductor, is summarized in the right half of Table 4. The coupling loss of the CNTF4, CSKO1, CSJA3-based CSMC1 and ITER PF5-based CSMC2 is 164.5, 49.1, 72.9 and 23.4 kJ, respectively. Similarly, the 5th time bucket (T5) and 8th time bucket (T18) are of the highest hysteresis loss.

4.3 AC loss comparison

From Table 4, the rate of magnetic field (dB/dt) is very low except the first time bucket when the CS2U simplified current is applied to coil, and applied current is relatively high. The total hysteresis loss is much larger than total coupling loss in the same type of CICC. Peak power of the conductor units in different types of CICC-based coil is given in Table 5. It can be seen that the coupling peak power of conductor units is much larger than hysteresis peak power of conductor units.

The smaller AC loss of CSKO1 than CSJA3 may have two reasons:

(1) The high matrix resistivity of internal-tin Nb_3Sn strands (CSKO1). The matrix of the internal-tin strand consists of more Sn than bronze-route Nb_3Sn strands (CSJA3), because the amount of Sn in the bronze-route Nb_3Sn strand is limited by the maximum solubility of Sn in Cu [23].
(2) The coupling time constant of CSKO1 is smaller than that of CSJA3 because the cable twist pitch is smaller; as the results of smaller coupling time constant, coupling power of CSKO1 conductor is smaller than that of CSJA3.

The peak power appears at the conductor unit where the magnetic field is up to the maximum value of CS model coil. From Fig. 1, the peak power in the CSMC1 is located at inner side of the equator plane, but for CSMC2, the peak power is located at the first layer of the top coil. In Table 5, the hysteresis peak powers of CNTF4, CSKO1 and CSJA3-based CSMC1 are 8.66, 18.54 and 21.33 W/m, respectively; the coupling peak powers are 78.25, 23.51 and 34.68 W/m, respectively; and the hysteresis and coupling peak powers of ITER PF5-based CSMC2 are 2.58 and 9.82 W/m, respectively. Interestingly, the coupling peak power is bigger than hysteresis peak power while coupling

Table 4 Hysteresis and coupling losses of the CSMC of different types of conductor

Items	Hysteresis loss (J)				Coupling loss (J)			
	CNTF4	CSKO1	CSJA3	ITER-PF5	CNTF4	CSKO1	CSJA3	ITER-PF5
T1	33,811	25,937	23,388	2899	8461	2525	3750	1204
T2	43,877	33,656	3035	376	1098	328	487	156
T3	21,178	16,246	14,649	1816	5300	1582	2349	754
T4	15,402	11,815	10,654	1321	3854	1150	1708	548
T5	145,881	111,908	100,911	12,508	36,508	10,894	16,180	5193
T6	5229	4011	3617	448	1309	391	580	186
T7	5862	4497	4055	503	1467	438	650	209
T8	5832	4474	4034	500	1460	436	647	208
T9	27,998	21,478	19,367	2401	70,076	2091	3105	997
T10	21,059	16,154	14,567	1806	5270	1573	2336	750
T11	9756	7484	6748	836	2441	729	1082	347
T12	14,604	11,203	10,102	1252	3655	1091	1620	520
T13	47,838	36,697	33,091	4102	11,972	3573	5306	1703
T14	2477	1900	1714	212	620	185	275	88
T15	126,238	96,839	87,323	10,824	31,592	9427	14,002	4493
T16	19,893	15,260	13,761	1706	4978	1486	2207	708
T17	0	0	0	0	0	0	0	0
T18	149,785	114,902	103,611	12,843	37,485	11,186	16,613	5331
T19	0	0	0	0	0	0	0	0
Total	657,231	504,171	454,630	56,353	164,478	49,082	72,894	23,394

Table 5 Peak power (W/m) of the conductor units

Items	CSMC1			PF5-based CSMC2
	CNTF4	CSKO1	CSJA3	
Hysteresis	8.66	18.54	21.23	2.58
Coupling	78.25	23.51	34.68	9.82
Total	86.91	52.05	55.91	12.40

loss is smaller than hysteresis loss. The reason is that there are many conductor units with low field amplitude B and low rate of the field (dB/dt) in a specific time bucket, which results in bigger coupling power and smaller hysteresis power in many other conductor units except the conductor unit where peak power occurs. In other words, in a full current cycle, there are few conductor units of which coupling peak power is bigger than hysteresis peak power. However, the hysteresis power of most of the 460 conductor units is bigger than coupling power. Finally, the hysteresis loss of CSMC is bigger than coupling loss for all the conductors.

5 Proposed experimental method

AC loss measurement is an important process throughout the design of a CS model coil [24–26]. For large-scale fusion magnetic coils, calorimetric method is used to measure the AC loss such as Sultan in Switzerland, ITER CS model coil and insert coil in Japan and KSTAR CS coil in Korea [27]. We developed the electrical AC loss measurement method for the CSMC [28], but the difficulties in measuring the AC loss include: (1) inductance of the large-scale coils is over 300 mH, so the inductive signal is too big to eliminate in general method; (2) the large operating current of the CSMC is non-sinusoidal and its measurement is tricky, as the frequently used Rogowski is not available in non-sinusoidal current environment.

To compensate the inductive signal of the CS model coil, the adjustable capacitor bank and compensation coil shall be used, as shown schematically in Fig. 4. The function of adjustable capacitor bank is to decrease the circuit impedance and increase the current. An adjustable capacitor bank is connected in series with sample coil, which can compensate part of inductive signal of sample coil. To further compensate the inductive signal of sample coil, we use adjustable compensation coil connected in anti-series with the sample coil. The adjustable compensation coil is wound by thousands of thin

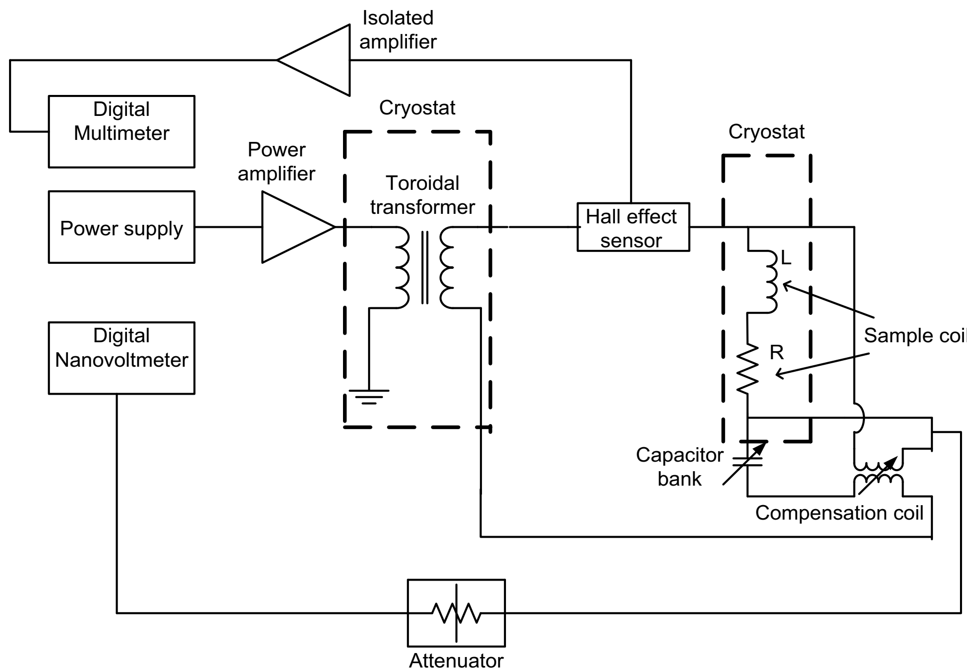

Fig. 4 Schematic principle and arrangement setup for measuring the AC loss of CFETR CS model coil

coppers (about $\Phi0.1$ mm) circles which can produce comparable inductive voltage signal to that of sample coil partly compensated by adjustable capacitor bank. To decrease the effect of magnetization error source on sample coil, adjustable compensation coil is located far from the CSMC field. In that case, the source of error from magnetization could be sufficiently small compared to the resistive component signal which is responsible for AC loss.

There are two measuring devices: (1) digital multimeter (DMM) to measure the voltage from Hall effect sensor to calibrate the operation current, and (2) digital nanovoltmeter to measure the voltage of sample coil after the capacitance adjustment, coil compensation, and attenuation. L and R are resistance and inductance of the CSMC, respectively. Since the changing rate of operating current of the CSMC is very high, along with big inductance, the voltage of CSMC is too big to be measured by the digital nanovoltmeter. To avoid overloading digital nanovoltmeter, the adjustable compensation coil is used to compensate the inductive signal of the CSMC and the compensated signal is further decreased by attenuator. In this system, current of the CSMC is calibrated by a Hall effect sensor, with a measuring range of from hundreds mA to tens of kA and a bandwidth from DC to hundreds of kHz. When a Hall effect sensor is exposed to perpendicular magnetic field B, a Hall voltage U_H is produced with a current I flowing into it, and $U_H = R_H BI/d$, where R_H is the coefficient of Hall effect sensor and d is thickness of the sensor. After proper decrease by isolated amplifier, U_H can be measured by DMM after the voltage signal of Hall effect sensor is attenuated by the isolated amplifier properly. All the process of transition and calculation is realized by LabVIEW and the coefficient of attenuator and isolated amplifier should be noticed in LabVIEW. Finally, the instantaneous value (INS) value of transport current and loss voltage component can be continuously measured, and the transport AC loss (W/m) is:

$$P_{ins} = \frac{I_{ins} V_{ins}}{L}, \tag{3}$$

$$P = \sum_T P_{ins}, \tag{4}$$

where P_{ins} and P is INS value of the loss and the loss in a full current cycle, respectively; I_{ins} is the INS value of transport current flowing through sample coil measured by Hall effect sensor; V_{ins} is INS value of resistive voltage component of the sample coil; and L is length of the sample coil.

6 Conclusions

Magnetic field distribution of the CSMC is simulated by COMSOL to verify the feasibility of design work, and the results well meet requirement of the safety assessment criteria of CFETR CS coil. AC hysteresis loss and AC coupling loss of CSMC1, based on different Nb_3Sn CICC, are calculated and compared. AC loss of CSMC2 based on NbTi-based ITER PF5 conductor is calculated. The losses of CSKO1- and CSJA3-based CSMC1 are much smaller than that of CNTF4 conductor. From the AC loss, ITER CS conductor is a better choice. A specific AC loss measurement system for the actual operation condition of being constructed CFETR CS model coil is proposed. These results can give a good reference for next step of R&D work and provide the valuable guidance for safe operation of CFETR CS model coil.

Acknowledgements The authors are thankful to all the members of CFETR CS model coil design team and ASIPP crew for providing some pictures. We would like to thank Arend Nijhuis from University of Twente and Zhenan Jiang from Victoria University of Wellington for measurement discussion.

References

1. B. Wan, S. Ding, J. Qian et al., Physics design of CFETR: determination of the device engineering parameters. IEEE Trans. Plasma Sci. **42**, 495 (2014). doi:10.1109/TPS.2013.2296939
2. Y. Wan, Mission of CFETR. in *Proceedings ITER Training Forum Second Workshop MFE Develop. Strategy*, Hefei, China, 1 (2012)
3. Y.T. Song, S.T. Wu, J.G. Li et al., Concept design of CFETR Tokamak machine. IEEE Trans. Plasma Sci. **42**, 503 (2014). doi:10.1109/TPS.2014.2299277
4. X. Liu, J. Zheng, Z. Luo et al., Conceptual design and analysis of CFETR magnets. in *The 25th Symposium on Fusion Engineering (SOFE). IEEE*, 1 (2013). doi: 10.1109/SOFE.2013.6635306
5. X.G. Liu, X.W. Wang, D.P. Yin et al., Electromagnetic optimization and preliminary mechanical analysis of the CFETR CS Model Coil. IEEE Trans. Plasma Sci. **44**, 1559 (2016). doi:10.1109/TPS.2016.2521892
6. J.G. Qin, T.J. Xue, B. Liu et al., Cabling technology of Nb_3Sn conductor for CFETR central solenoid model coil. IEEE Trans. Appl. Supercond. **26**, 1 (2016). doi:10.1109/TASC.2016.2525923
7. H. Jin, Y. Wu, F. Long et al., Mechanical properties of preliminary designed insulation for CFETR CSMC. IEEE Trans. Appl. Supercond. **26**, 1 (2016). doi:10.1109/TASC.2016.2518490
8. Y.L. Yang, Y. Wu, B. Liu, A new numerical model for the quench simulation in CFETR CSMC conductor. IEEE Trans. Appl. Supercond. **26**, 1 (2016). doi:10.1109/TASC.2016.2532461
9. A. Nijhuis, N.H.W. Noordman, O.A. Shevchenko et al., Electromagnetic and mechanical characterization of ITER CS–MC conductors affected by transverse cyclic loading, part 1: coupling current losses. IEEE Trans. Appl. Supercond. **9**, 1069 (1999). doi:10.1109/77.783482
10. W. Zhou, X.Y. Fang, J. Fang et al., DC performance and AC loss of cable-in-conduit conductors for International thermonuclear experimental reactor. Nucl. Sci. Tech. **27**, 1 (2016). doi:10.1007/s41365-016-0061-2
11. W. Chung, Y. Chu, S. Lee et al., Analysis of the KSTAR central solenoid model coil experiment. IEEE Trans. Appl. Supercond. **17**, 1338 (2007). doi:10.1109/TASC.2007.899989
12. Y. Shi, Y. Wu, Q.W. Hao et al., The AC loss evaluation of central solenoid model coil for CFETR. Fusion Eng. Des. **107**, 100 (2016). doi:10.1016/j.fusengdes.2016.03.070
13. A. Devred, I. Backbier, D. Bessette et al., Status of ITER conductor development and production. IEEE Trans. Appl. Supercond. **22**, 4804909 (2012). doi:10.1109/TASC.2012.2182980
14. B. Liu, Y. Wu, A. Devred et al., Conductor performance of TFCN4 and TFCN5 samples for ITER TF coils. IEEE Trans. Appl. Supercond. **25**, 1 (2015). doi:10.1109/TASC.2014.2376931
15. D. Bessette, Design of a cable-in-conduit conductor to withstand the 60 000 electromagnetic cycles of the ITER central solenoid. IEEE Trans. Appl. Supercond. **24**, 1 (2014). doi:10.1109/TASC.2013.2282399
16. L. Feng, W. Yu, L. Fang et al., Manufacture and acceptance test of the full size ITER PF5 conductor sample. IEEE Trans. Appl. Supercond. **22**, 4805404 (2012). doi:10.1109/TASC.2011.2175432
17. F. Gauthier, 15MA CS thermal hydraulic analysis with the SuperMagnet code. in ITER_D_APUB8, v 1.1, pp: 35–36, Aug. 2012
18. A.M. Campbell, A general treatment of losses in multifilamentary superconductors. Cryogenics **22**, 3 (1982). doi:10.1016/0011-2275(82)90015-7
19. M.N. Wilson, *Superconducting Magnets* (Oxford Science Publications, London, 1987), pp. 177–192
20. L. Bottura, B. Bordini, J_c (B, T, ε) parameterization for the ITER Nb_3Sn production. IEEE Trans. Appl. Supercond. **19**, 1521 (2009). doi:10.1109/TASC.2009.2018278
21. L. Bottura, A practical fit for the critical surface of NbTi. IEEE Trans. Appl. Supercond. **10**, 2000 (1054). doi:10.1109/77.828413
22. B. Xiao, P. Weng, Integrated analysis of the electromagnetical, thermal, fluid flow fields in a Tokamak. Fusion Eng. Des. **81**, 1549 (2006). doi:10.1016/j.fusengdes.2005.10.013
23. T. Suwa, Y. Nabara, H. Ozeki et al., Analysis of internal-Tin Nb_3Sn conductors for ITER central solenoid. IEEE Trans. Appl. Supercond. **25**, 4201704 (2015). doi:10.1109/TASC.2014.2376990
24. Y. Takahashi, K. Matsui, K. Nishii et al., AC loss measurement of 46 kA-13T Nb_3Sn conductor for ITER. IEEE Trans. Appl. Supercond. **11**, 1546 (2001). doi:10.1109/77.920071
25. Y. Wang, X. Guan, J. Dai, Review of AC loss measuring methods for HTS tape and unit. IEEE Trans. Appl. Supercond. **24**, 1 (2014). doi:10.1109/TASC.2014.2340457
26. Z. Jiang, N. Amemiya, An experimental method for total AC loss measurement of high T_c superconductors. Supercond. Sci. Technol. **17**, 371 (2004). doi:10.1088/0953-2048/17/3/014
27. S. Lee, Y. Chu, W.H. Chung et al., AC loss characteristics of the KSTAR CSMC estimated by pulse test. IEEE Trans. Appl. Supercond. **16**, 771 (2006). doi:10.1109/TASC.2006.870541
28. W. Zhou, J. Fang, B. Liu et al., AC loss analysis of central solenoid model coil for China fusion engineering test reactor. IEEE Trans. Appl. Supercond. **26**, 5900505 (2016). doi:10.1109/TASC.2016.2580564